

## Supporting Information

### Electropolymerization of $\beta$ -cyclodextrin onto multi-walled carbon nanotube composite films for enhanced selective detection of uric acid

Mulugeta B. Wayu, Luke T. DiPasquale, Margaret A. Schwarzmann, Samuel D. Gillespie, and Michael C. Leopold \*

#### Contents:

- ▶ Instrumentation/Procedural Details of Microscopy and Spectroscopic Characterization of Films
- ▶ **Figure SI-1.** (A) cyclic voltammetry; (B) Differential pulse voltammetry (cathodic sweep) and (C) chronocoulometry (CC) of 5 mM potassium ferricyanide (0.5 M KCl) at (a) bare GCE, (b) Nafion and (c) Nafion–MWCNT nanocomposite modified GCE.
- ▶ **Table SI-1.** Summary of results from chronocoulometry experiments to determine electroactive surface area of modified glassy carbon electrodes.
- ▶ **Figure SI-2:** Cyclic voltammetry of a) GCE/HPU, b) GCE/b-CD/HPU, c) HPU/Nafion–MWCNT/GCE and d) GCE/Nafion–MWCNT/ $\beta$ -CD/HPU electrochemical sensors in 65.55 mM PBS (pH = 7.0) A) without and B) with 1mM UA.
- ▶ **Figure S-3:** Representative amperometric I-t curve and corresponding calibration curve (**inset**) during successive 0.1 mM injections of uric acid at bare glassy carbon electrode coated with HPU.
- ▶ **Figure SI-4:** AFM images of pristine MWCNT
- ▶ **Figure SI-5:** TEM image of A) pristine MWCNT, B)  $\beta$ -CD, C) Nafion–MWCNT and (D) Nafion–MWCNT/  $\beta$ -CD
- ▶ **Figure SI-6.** The electropolymerization graphs of b-CD at (a) bare GCE and (c) Nafion–MWCNT nanocomposite modified GCE in 65.55 mM PBS (pH = 7.0) containing 0.01 M  $\beta$ -CD. **2b** and **2d** shows the last (10<sup>th</sup>) scans during the electropolymerization of  $\beta$ -CD.
- ▶ **Figure SI-7:** The sensitivity of a) GCE/Nafion–MWCNT/  $\beta$ -CD/HPU, and b) GCE/  $\beta$ -CD/HPU towards the oxidation of UA at +0.30 V versus the number of  $\beta$ -CD polymerization cycles between – 0.8 and 1.3 V at sweep rate of 100 mV.s<sup>-1</sup>
- ▶ **Figure S-8:** Representative amperometric I-t curves and corresponding calibration curves (**inset**) during successive 0.1 mM injections of uric acid at a) GCE/Nafion–MWCNT/ $\alpha$ -CD/HPU, b) GCE/Nafion–MWCNT/ $\gamma$ -CD/HPU and c) GCE/Nafion–MWCNT/  $\beta$ -CD/HPU electrochemical sensors.
- ▶ **Figure S-9:** (A) cyclic voltammetry of 5 mM potassium ferricyanide (0.5 M KCl) at (a) GCE/  $\beta$ -CD, (b) bare GCE, (c) GCE/Nafion–MWCNT/  $\beta$ -CD and (d) GCE/Nafion-MWCNT; (B) Typical amperometric I-t curves of GCE/Nafion-MWCNT/HPU electrochemical sensor during injections of common interferent species and UA and a graphical summary (**Inset**) of selectivity coefficients for acetaminophen (AP), ascorbic acid (AA), NaNO<sub>2</sub>, oxalic acid (OA), and glucose (Glu) at a) +0.65 and b) +0.30 V vs Ag/AgCl.
- ▶ **Table SI-2:** Comparison of Amperometric Uric Acid Biosensor Performance Parameters – Literature Comparison (with References)

## **Instrumentation/Procedural Details of Microscopy and Spectroscopic Characterization of Films**

**Transmission Electron Microscopy (TEM).** MWCNT structure and Nafion encapsulation of the NTs was supported visually with TEM (JEOL 1010) characterization as was the presence of  $\beta$ -CD within the films. Samples of CNT/Nafion films with electropolymerized  $\beta$ -CD were removed from button electrodes, and were dissolved in ethanol before casting on a TEM grid. Separate TEM grids (Formvar/Carbon 400 mesh, Cu, Electron Microscopy Sciences) were created with specific combinations of the materials comprising the film systems were prepared as were samples of the individual components of the film systems.

**Scanning Electron Microscopy (SEM).** Nafion-MWCNT/ $\beta$ -CD were also characterized with SEM (JEOL 6360). Complete films which included all of the individual components were removed from the electrode surface and dissolved in ethanol before drop casting onto the SEM aluminum stud platform.

**Atomic Force Microscopy (AFM).** MWCNT were dispersed using dimethyl formamide or methylene chloride on either silicon or gold substrates that were previously cleaned with sulfuric acid (0.1 M), rinsed ( $H_2O$ ), and dried under a stream of nitrogen before being imaged with the AFM (Asylum).

**IR.** FTIR spectroscopy was conducted using a Thermo Scientific Nicolet Model iS10 FTIR equipped with a diamond SMART iTX HATR sample accessory.

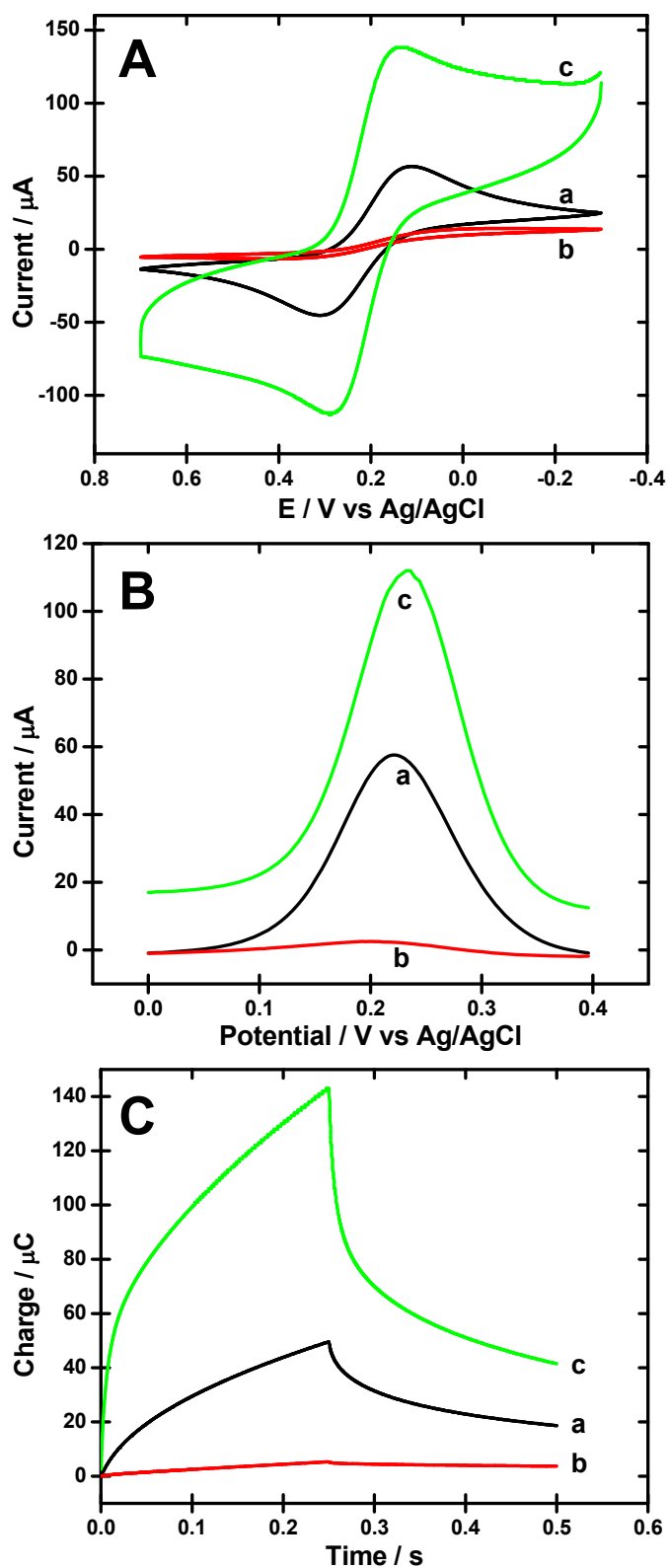


**Figure SI-1.** (A) cyclic voltammetry; (B) Differential pulse voltammetry (cathodic sweep) and (C) chronocoulometry (CC) of 5 mM potassium ferricyanide (0.5 M KCl) at (a) bare GCE, (b) Nafion and (c) Nafion–MWCNT nanocomposite modified GCE. **DPV parameters:** Potential window =  $0 \leftrightarrow +0.4$  V; Pulse width = 0.05 s; Amplitude = 0.05 V; Period = 0.5 s; Sensitivity 1E-4 A/V

**Table SI–1.** Chronocoulometry (CC), Cyclic Voltammetry (CV) and Differential Pulse Voltammetry (DPV) Summary for Cathodic Waves of 5 mM  $[\text{Fe}(\text{CN})_6]^{3-/4-}$  (0.5 M KCl) before and after modification of GCEs with Nafion and Nafion–MWCNT nanocomposite.

Electrode Type	Average Area ( $\text{cm}^2$ ) from CC	CV Average $I_{\text{p,c}}$ ( $\mu\text{A}$ ) <sup>a</sup>	CV Average $I_{\text{p,c}}$ ( $\mu\text{A}$ ) <sup>b</sup>	CV Average $I_{\text{p,c}} - \text{BG}$ ( $\mu\text{A}$ ) <sup>c</sup>	DPV Average $I_{\text{p,c}}$ ( $\mu\text{A}$ ) <sup>d</sup>
GCE	$0.071 \pm 0.003$	$59.7 \pm 5.0$	$55.6 \pm 6.8$	$55.60 \pm 6.6$	$50.9 \pm 11$
GCE/Nafion	$0.007 \pm 0.003$	$11.3 \pm 3.5$	$6.74 \pm 1.90$	$6.76 \pm 1.9$	$3.49 \pm 0.8$
GCE/Nafion–MWCNT	$0.149 \pm 0.006$	$108 \pm 14$	$85.70 \pm 14.0$	$89.4 \pm 14$	$85.3 \pm 10$

**Notes:** – Uncertainty values listed represent standard deviation (n=3).

<sup>a</sup> Faradaic and non–Faradaic (charging) peak current ( $i_{\text{p,c}}$ );

<sup>b</sup> Isolated Faradaic current from individual peak analysis;

<sup>c</sup> Isolated Faradaic current after background subtraction of same scans in 0.5 M KCl supporting electrolyte;

<sup>d</sup> Isolated Faradaic current from individual peak analysis;

**DPV parameters:** Potential window =  $0 \leftrightarrow +0.4$  V; Pulse width = 0.05 s; Amplitude = 0.05 V; Period = 0.5 s; Sensitivity 1E–4 A/V

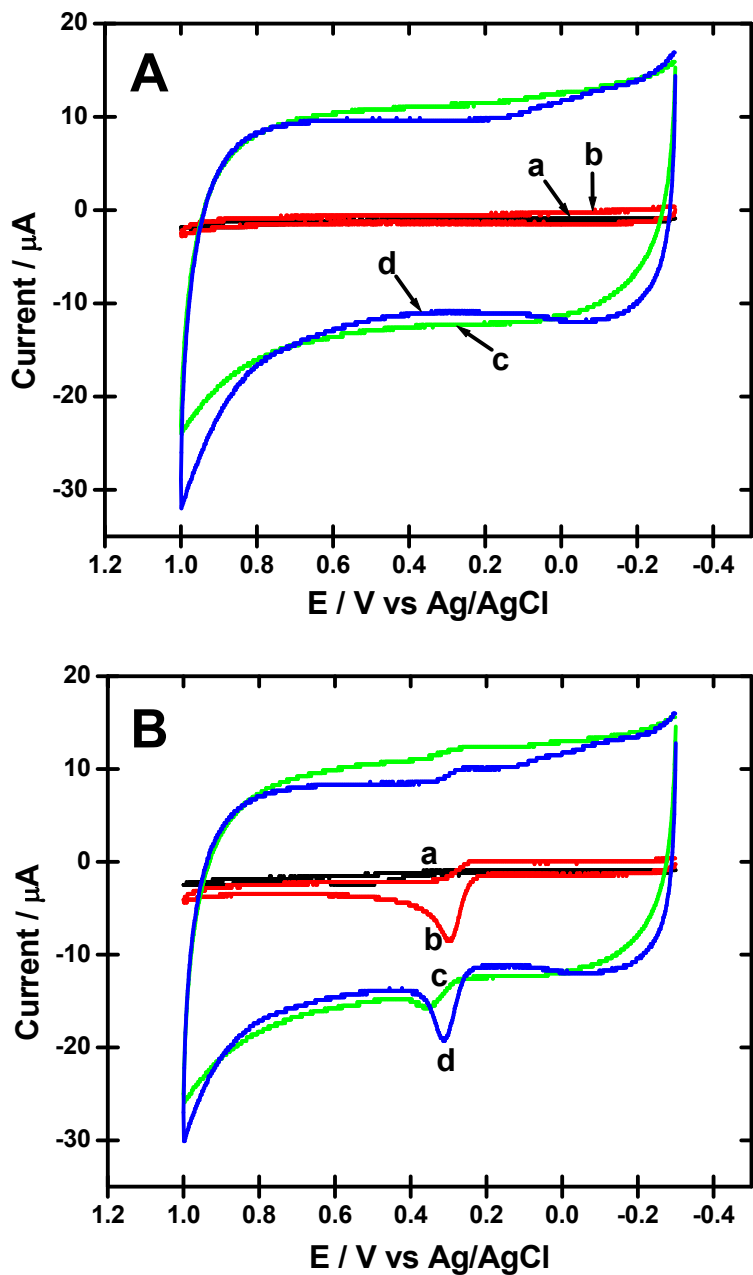


**Figure SI-2:** Cyclic Voltammograms of a) GCE/HPU, b) GCE/ $\beta$ -CD/HPU, c) GCE/Nafion–MWCNT/HPU and d) GCE/Nafion–MWCNT/ $\beta$ -CD/HPU electrochemical sensors in 65.55 mM PBS (pH = 7.0) (A) without (background) and (B) with 1 mM UA.

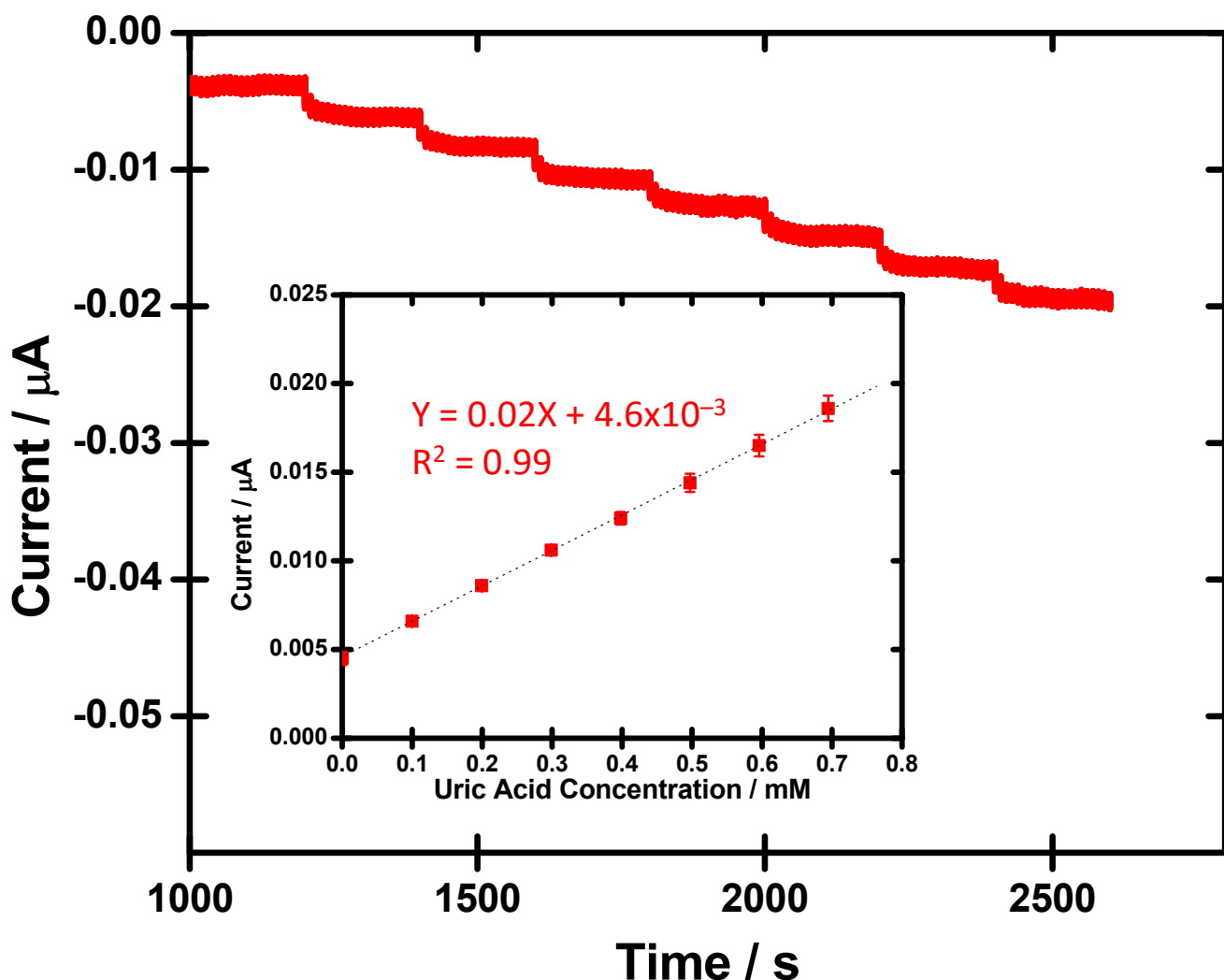


**Figure S-3:** Representative amperometric I-t curve and corresponding calibration curve (inset) during successive 0.1 mM injections of uric acid at bare glassy carbon electrode coated with HPU. Note: In some cases, standard error bars are smaller than markers for average value ( $n = 6$ ).

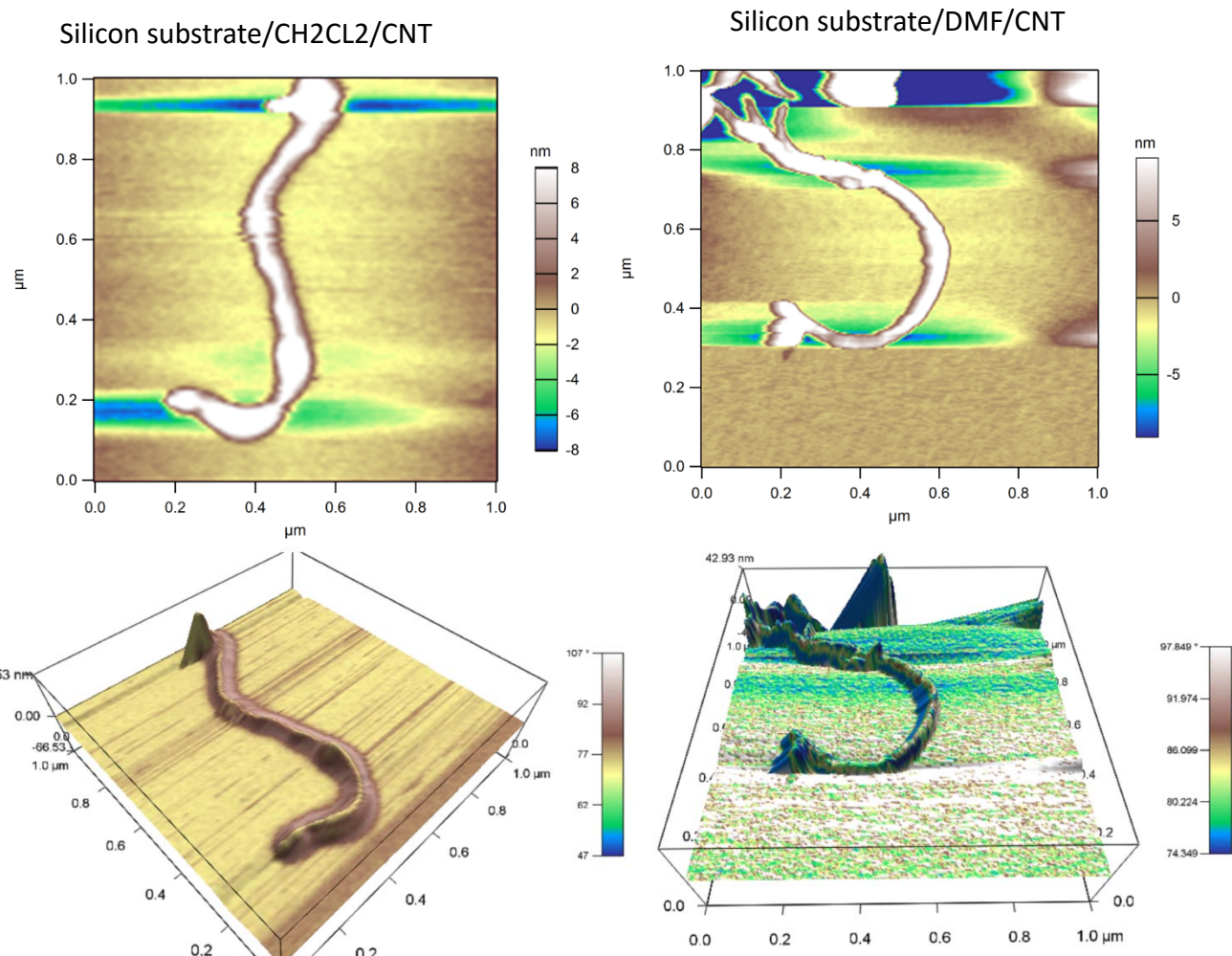


**Figure SI-4:** AFM images of pristine MWCNT dispersed in dichloromethane and dimethylformamide (DMF).

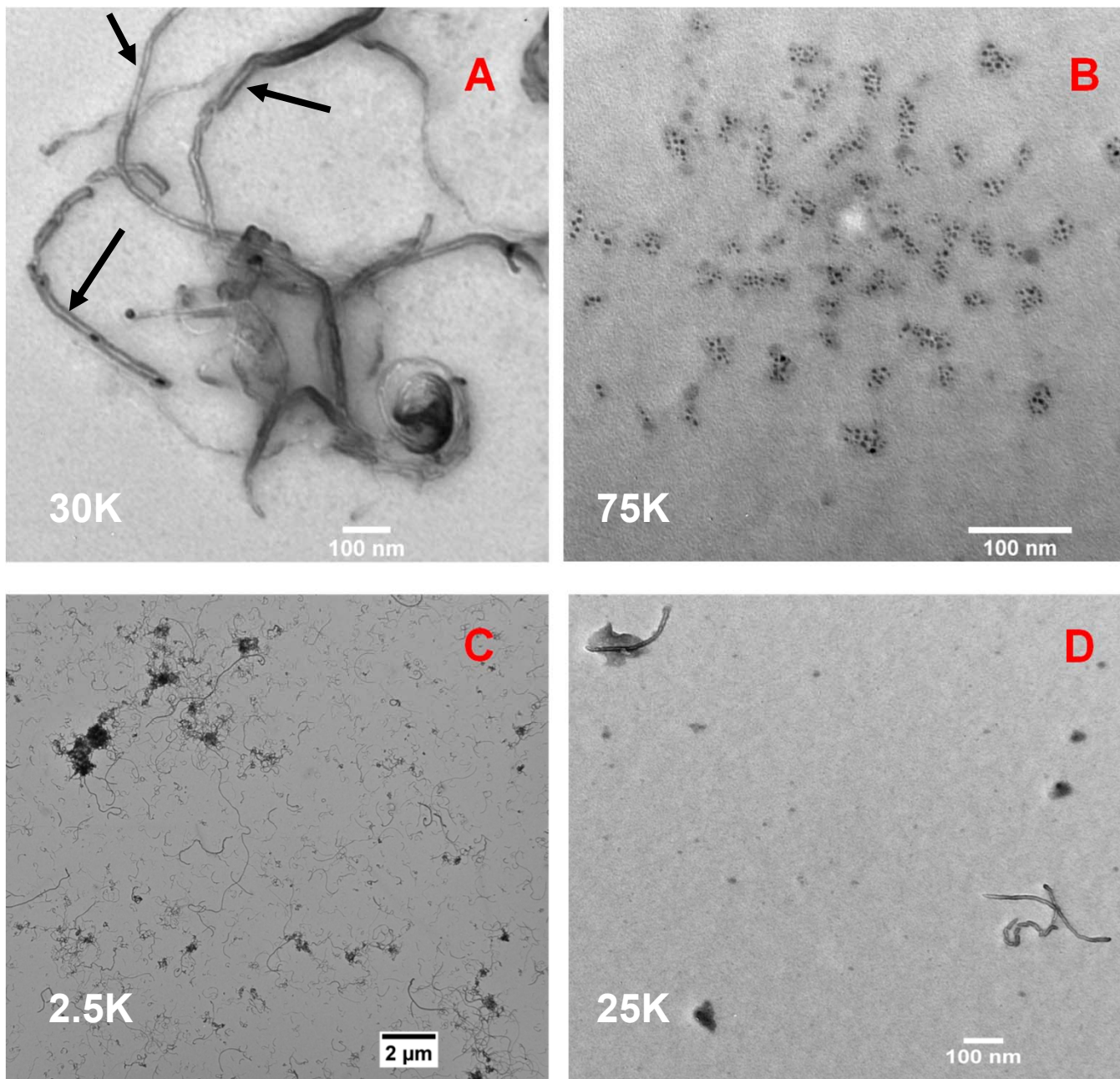


**Figure SI-5:** TEM image of **A)** pristine MWCNT, **B)**  $\beta$ -CD, **C)** Nafion-MWCNT and **(D)**  $\beta$ -CD/Nafion-MWCNT

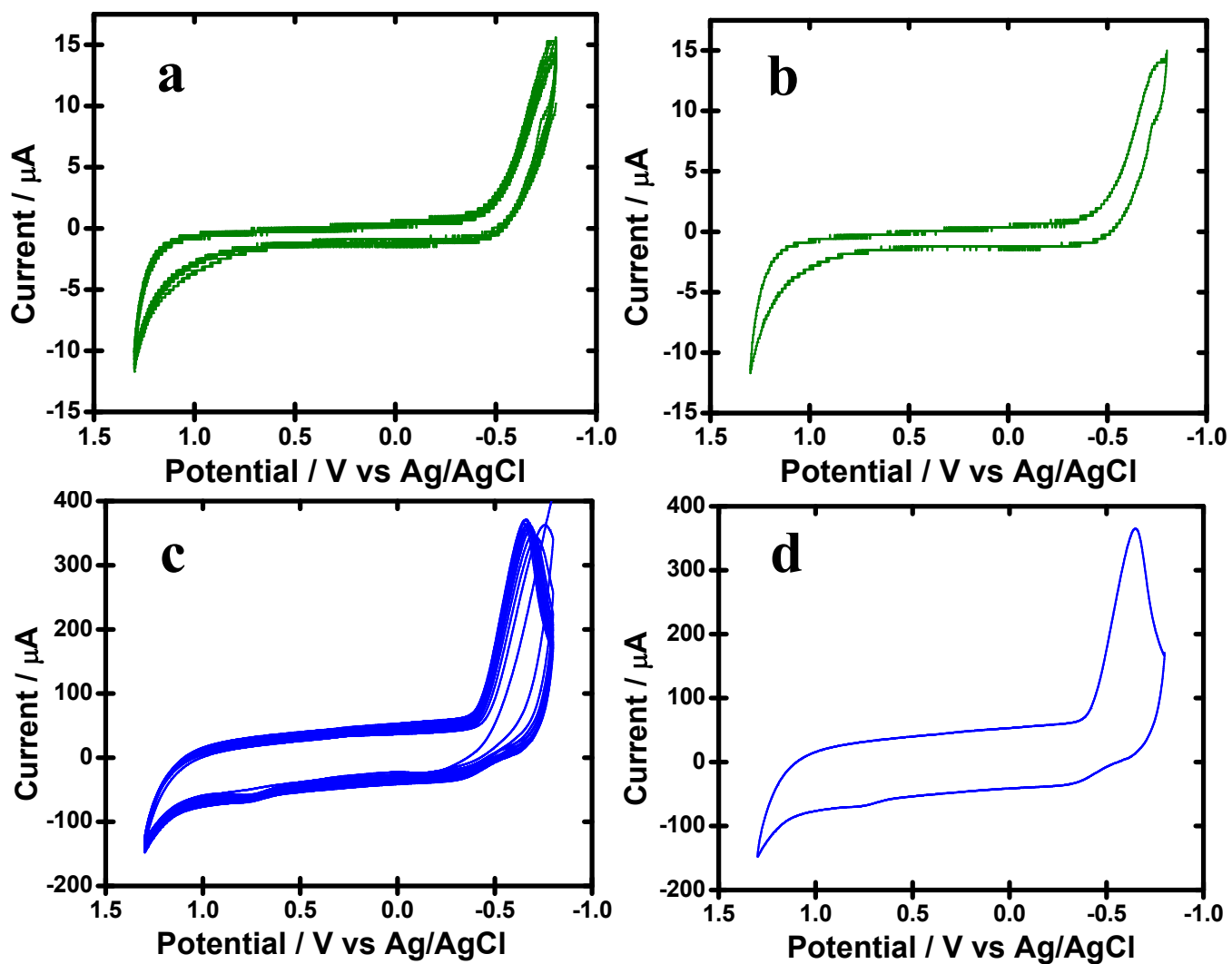


**Figure SI-6.** The electropolymerization graphs of  $\beta$ -CD at (a) bare GCE and (c) Nafion–MWCNT nanocomposite modified GCE in 65.55 mM PBS (pH = 7.0) containing 0.01 M  $\beta$ -CD. 2b and 2d shows the last (10<sup>th</sup>) scans during the electropolymerization of  $\beta$ -CD. When compared to bare GCE, the observed ~20-fold increase in the peak current between -0.4 and -0.8 V vs Ag/AgCl for Nafion–MWCNT modified GCE, is attributed to the large surface area effect contributed by MWCNT to accommodate large amounts of  $\beta$ -CD.

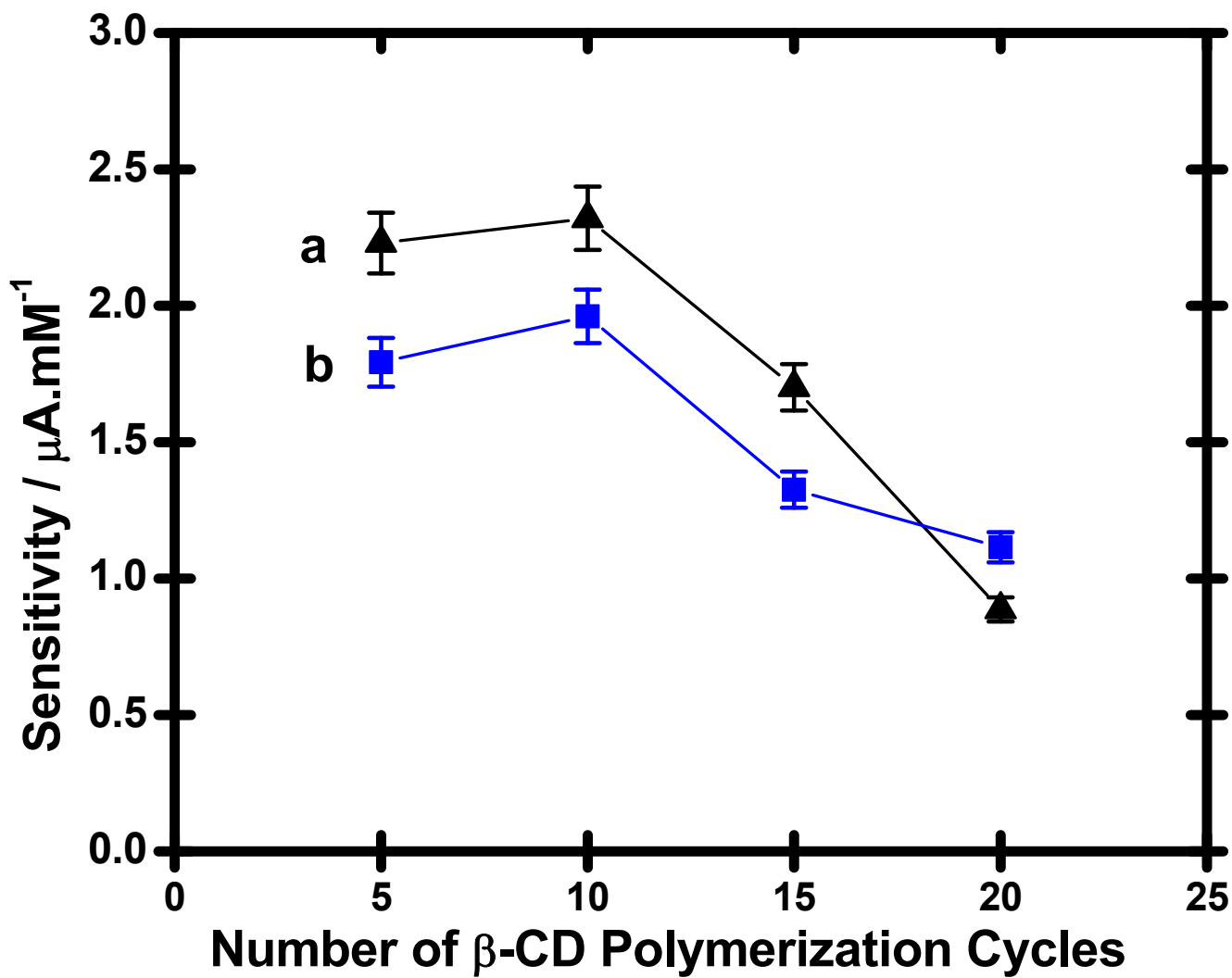


**Figure SI-7:** The sensitivity of **a)** GCE/Nafion–MWCNT/ $\beta$ -CD/HPU, and **b)** GCE/ $\beta$ -CD/HPU towards the oxidation of UA at +0.30 V versus the number of  $\beta$ -CD polymerization cycles between –0.8 and 1.3 V at sweep rate of 100  $\text{mV.s}^{-1}$

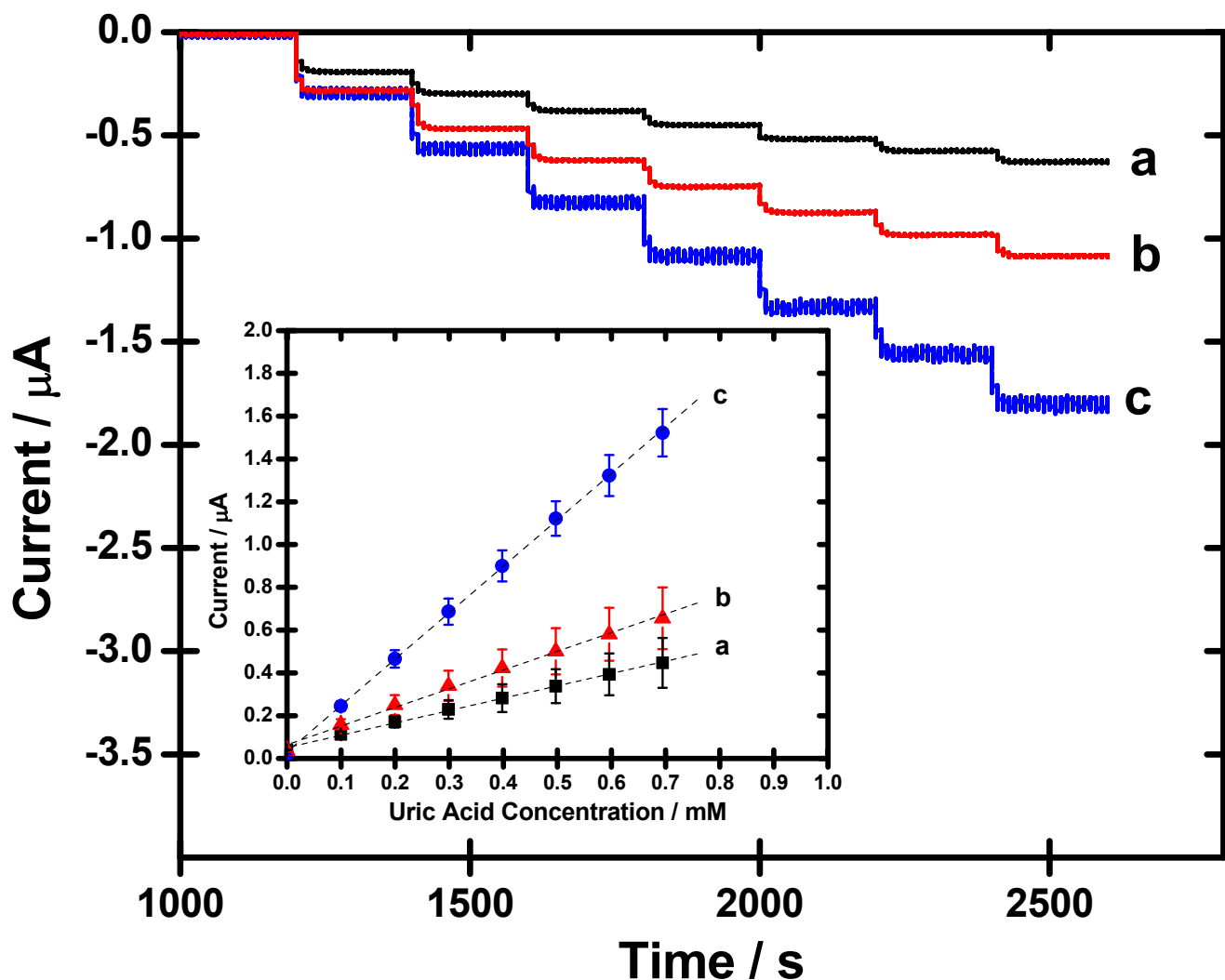


**Figure S-8:** Representative amperometric I-t curves and corresponding calibration curves (inset) during successive 0.1 mM injections of uric acid at **a)** GCE/Nafion–MWCNT/ $\alpha$ -CD/HPU, **b)** GCE/Nafion–MWCNT/ $\gamma$ -CD/HPU and **c)** GCE/Nafion–MWCNT/ $\beta$ -CD/HPU electrochemical sensors. Note: In some cases, standard error bars are smaller than markers for average value ( $n = 3$ ).

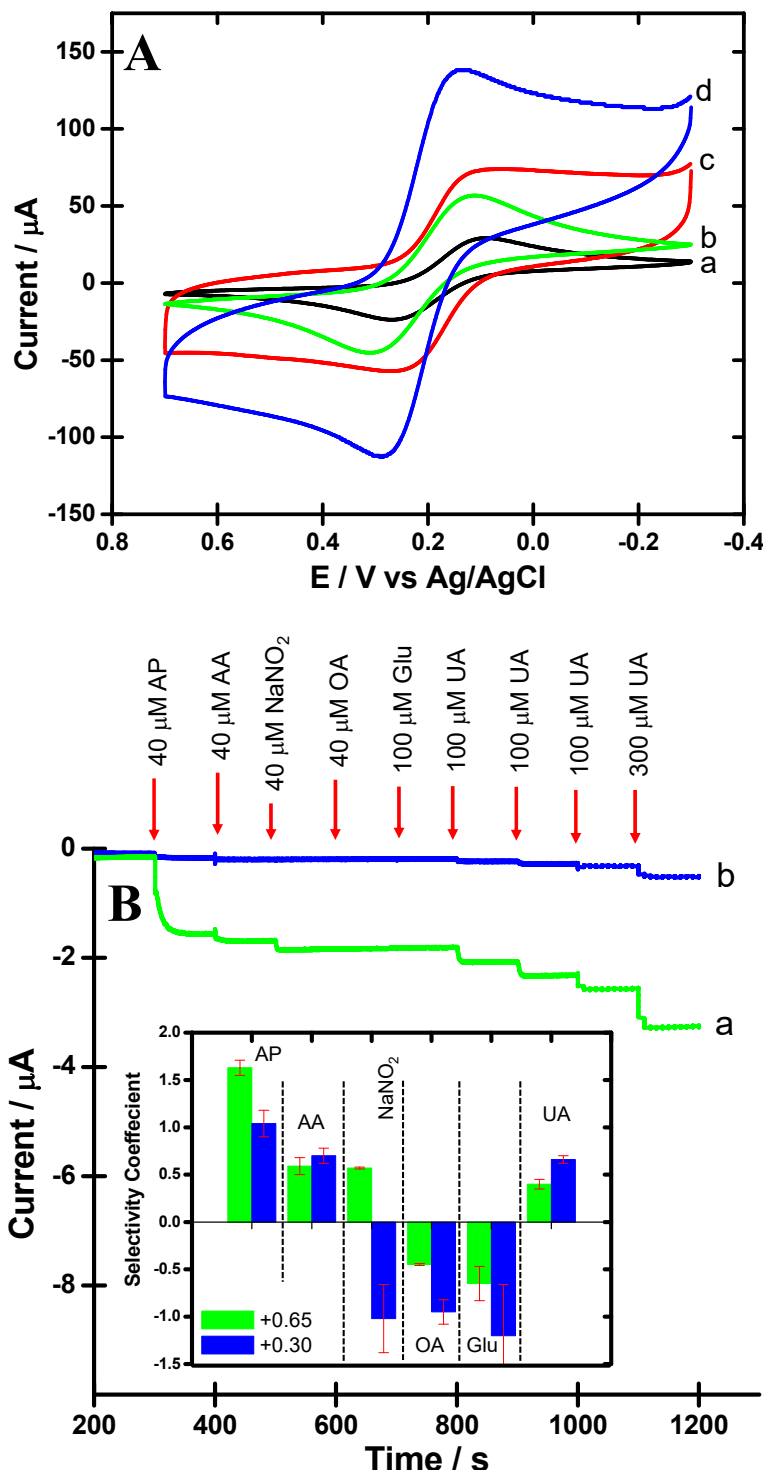


**Figure S-9:** (A) cyclic voltammetry of 5 mM potassium ferricyanide (0.5 M KCl) at (a) GCE/β-CD, (b) bare GCE, (c) GCE/Nafion-MWCNT/β-CD and (d) GCE/Nafion-MWCNT; (B) Typical amperometric I-t curves of GCE/Nafion-MWCNT/HPU electrochemical sensor during injections of common interferent species and UA and a graphical summary (Inset) of selectivity coefficients for acetaminophen (AP), ascorbic acid (AA),  $\text{NaNO}_2$ , oxalic acid (OA), and glucose (Glu) at a) +0.65 and b) +0.30 V vs Ag/AgCl. Note: In some cases, standard error bars are smaller than markers for average value ( $n=3$ ).

**Table SI-2:** Comparison of Amperometric Uric Acid Biosensor Performance Parameters – Literature Comparison (References listed next page)

System	Type	WE	Sensitivity	Response Time	Linear Range <sup>a</sup>	Dynamic Range <sup>a</sup>	LOD	Stability	Ref <sup>c</sup>
		(nA/ $\mu$ M)	(s)	( $\mu$ M)	( $\mu$ M)	( $\mu$ M) <sup>b</sup>	( $\mu$ M) <sup>b</sup>		
Nafion-MWCNT/ $\beta$ -CD/HPU	Direct	GCE	2.11 <sub>±0.29</sub>	5.38 <sub>±0.33</sub>	700	700	12	2 weeks	d.
Pt/PtB/MPC-HMTES*/HMTES/PL-A/HPU	1 <sup>st</sup> G	Pt	0.97 <sub>±0.11</sub>	15	700	700	15	5 days	1.
Pt/HMTES*/HMTES/PL-A/PU	1 <sup>st</sup> G	Pt	0.78 <sub>±0.11</sub>	10.0 <sub>±5.3</sub>	700	700	5.0 <sub>±2.4</sub>	>10 days	2.
<b>Selected Multi-walled Carbon Nanotubes Based UA Sensors From Literature</b>									
Au/c-MWCNT/AuNP/UO <sub>x</sub>	1 <sup>st</sup> G	Au	-	7	800	-	0.01 mM	120 days	3.
Au/MWCNTs	Direct	Au	92.19	2	1800	-	0.1 $\mu$ M/mM	2 weeks, 10% decrease	4.
ITO/MWCNT/PANI/UO <sub>x</sub>	1 <sup>st</sup> G	ITO	-	8	600	600	5	90 days	5.
Au/MWCNT/AuNP/UO <sub>x</sub>	1 <sup>st</sup> G	Au	-	7	800	800	10	120 days	6.
GCE/PVDF/GEL/c-MWCNT/UO <sub>x</sub>	2 <sup>nd</sup> G	GCE	-	40	710	-	2.3x10 <sup>-8</sup> M	Day 1-10; 30% decrease; Day 11-35; 50% decrease	7.
GCE/MWCNT-HoFNPs	Direct	GCE	-	-	0.2-500	0.2-500	0.16	6 months	8.
$\beta$ -CD/CNT/GE	Direct	GE	2.7	-	0.5-50	0.5-50	0.2	4 days	9.

**Notes:** \* indicates UO<sub>x</sub> doped layer; **a.** Typical upper limit of range listed; **b.** Limit of detection (L.O.D.) is the concentration required to elicit a sensor response ( $3\sigma_{BL}/\beta_1$ ); **c.** Comparative references (examples) listed next page with **(d.)** current work; **Additional notes:** MWCNT: multi-walled carbon nanotubes;  $\beta$ -CD: beta cyclodextrin; HPU: hydrothane polyurethane; GCE: glassy carbon electrode; PtB: Platinum black; MPC: monolayer-protected cluster; HMTES: hydroxymethyltriethoxysilane; PL-A: polyluminol/polyaniline; 1<sup>st</sup> G: 1<sup>st</sup> generation (indirect); ITO: indium tin-oxide; 2<sup>nd</sup> G: 2<sup>nd</sup> generation (mediated); PANI: polyaniline; AuNP: Gold nanoparticles; PVF: Poly(vinylferrocene); HoFNPs: holmium Fluoride nanoparticles; GE: graphite electrode.

**Table SI-2 References**

1. Wayu, M. B.; Pannell, M. J.; Leopold, M. C.: Layered Xerogel Films Incorporating Monolayer-Protected Cluster Networks on Platinum-Black-Modified Electrodes for Enhanced Sensitivity in First-Generation Uric Acid Biosensing. *ChemElectroChem* **2016**, *3*, 1245-1252.
2. Conway, G. E.; Lambertson, R. H.; Schwarzmann, M. A.; Pannell, M. J.; Kerins, H. W.; Rubenstein, K. J.; Dattelbaum, J. D.; Leopold, M. C.: Layer-by-layer design and optimization of xerogel-based amperometric first generation biosensors for uric acid. *J. Electroanal. Chem.* **2016**, *775*, 135-145.
3. Chanhan, N.; Pundir, C. An Amperometric Uric Acid Biosensor Based on Multiwalled Carbon Nanotube-Gold Nanoparticle Composite. *Anal. Biochem.* **2011**, *413*, 97-103.
4. Wang, J.; Zhang, W. Sputtering Deposition of Gold Nanoparticles onto Vertically Aligned Carbon Nanotubes for Electroanalysis of Uric Acid. *J. Electroanal. Chem.* **2011**, *654*, 79-84.
5. Bhambi, M.; Sumana, G.; Malhotra, B. D.; Pundir, C. S.: An Amperometric Uric Acid Biosensor Based on Immobilization of Uricase onto Polyaniline-multiwalled Carbon Nanotube Composite Film. *Artif. Cells, Blood Substitutes Biotechnol.* **2010**, *38*, 178-185.
6. Chauhan, N.; Pundir, C. S.: An amperometric uric acid biosensor based on multiwalled carbon nanotube-gold nanoparticle composite. *Anal. Biochem.* **2011**, *413*, 97-103.
7. Erden, P.; Kacar, C.; Ozturk, F; Kilic, E. Amperometric Uric Acid Biosensor Based on Poly(vinylferrocene)-Gelatin-Carboxylated Multiwalled Carbon Nanotube Modified Glassy Carbon Electrode. *Talanta* **2015**, *134*, 488-495.
8. Noroozifar, M.; Khorasani-Motlagh, M.; Jahromi, F. Z.; Rostami, S.: Sensitive and selective determination of uric acid in real samples by modified glassy carbon electrode with holmium fluoride nanoparticles/multi-walled carbon nanotube as a new biosensor. *Sens. Actuators B: Chem.* **2013**, *188*, 65-72.
9. Wang, Z.; Wang, Y.; Luo, G.: A selective voltammetric method for uric acid detection at [small beta]-cyclodextrin modified electrode incorporating carbon nanotubes. *Analyst* **2002**, *127*, 1353-1358.